Analytical Elastic Stiffness Model for 3D Woven Orthogonal Interlock Composites

Saul Buchanan, Alexander Grigorash, Edward Archer, Alistair Mcilhagger, Justin Quinn, Graeme Stewart

Accepted Manuscript

Analytical Elastic Stiffness Model for 3D Woven Orthogonal Interlock Composites

Saul Buchanan, Alexander Grigorash, Edward Archer, Alistair McIlhagger, Justin Quinn, Graeme Stewart

PII: S0266-3538(10)00203-4
DOI: 10.1016/j.compscitech.2010.05.019
Reference: CSTE 4724

To appear in: *Composites Science and Technology*

Received Date: 10 December 2009
Revised Date: 14 May 2010
Accepted Date: 23 May 2010

Please cite this article as: Buchanan, S., Grigorash, A., Archer, E., McIlhagger, A., Quinn, J., Stewart, G., Analytical Elastic Stiffness Model for 3D Woven Orthogonal Interlock Composites, *Composites Science and Technology* (2010), doi: 10.1016/j.compscitech.2010.05.019

Title: Analytical Elastic Stiffness Model for 3D Woven Orthogonal Interlock Composites

Article Type: Full Length Article

Section/Category: Mechanics, modelling and analysis

Keywords: A. Textile composites; C. Modelling; C. Elastic properties; 3D woven composites

Corresponding Author: Dr Saul Buchanan; s.buchanan@qub.ac.uk

Corresponding Author's Institution: Engineering Composite Research Centre, University of Ulster, Jordanstown, Newtownabbey, BT37 0QB

First Author: Saul Buchanan

Order of Authors: Saul Buchanan; Alexander Grigorash; Edward Archer; Alistair McIlhagger; Justin Quinn; Graeme Stewart

Author Details:

Alexander Grigorash; School of Computing and Mathematics, University of Ulster, Jordanstown, Newtownabbey, BT37 0QB

Edward Archer; Engineering Composite Research Centre, University of Ulster, Jordanstown, Newtownabbey, BT37 0QB

Alistair McIlhagger; Engineering Composite Research Centre, University of Ulster, Jordanstown, Newtownabbey, BT37 0QB

Justin Quinn; Engineering Composite Research Centre, University of Ulster, Jordanstown, Newtownabbey, BT37 0QB

Graeme Stewart; Engineering Composite Research Centre, University of Ulster, Jordanstown, Newtownabbey, BT37 0QB

Abstract: This research presents the development of an analytical model to predict the elastic stiffness performance of orthogonal interlock bound 3D woven composites as a consequence of altering the weaving parameters and constituent material types.
The present approach formulates expressions at the micro level with the aim of calculating more representative volume fractions of a group of elements to the layer. The rationale in representing the volume fractions within the unit cell more accurately was to improve the elastic stiffness predictions compared to existing analytical modelling approaches.
The models developed in this work show good agreement between experimental data and improvement on existing predicted values by models published in literature.

1. Introduction

Three-dimensionally (3D) woven composites have been identified as a class of material that have potential performance and manufacturing benefits compared to traditional two-dimensional (2D) laminate composites for structural applications[1-6]. The 3D weaving process controls the placement of reinforcing tows in the X, Y, and Z axis directions. A designer can potentially tailor the performance of the weave architecture to the specific requirements of the application by altering the weaving parameters. There are numerous combinations of weaving parameters that could be selected each of which imparts a different mechanical performance. A lack of understanding currently exists as to the effect on the mechanical performance as a consequence of altering the weaving parameters. To help realise the potential benefits of 3D woven composites, the designer must be facilitated with modelling tools that allows them to quickly evaluate the effect of weaving parameters on the geometric characteristics and mechanical performance.

In literature there are two approaches to facilitate this aim i.e. Finite Element (FE) and analytical models. The FE approaches have the potential to encapsulate more complexities of the 3D woven composite than analytical methods but are generally too computationally and time intensive[7]. This would make such methods unsuitable when trying to assess quickly numerous permutations of 3D weave architecture and the consequences of altering the constituent materials and weaving parameters on the mechanical performance of the composite. Therefore, a clear need for accurate analytically based approaches is still necessary. There are numerous analytically based models developed to model the mechanical performance of 3D woven composites[8-14]. These analytical approaches use similar principles to formulate relationships based on the spatial orientation of unidirectional tows in the unit cell or a small representative volume of the composite[15,16]. The accuracy of the predicted mechanical properties is only as accurate as the inputted geometric definition/description of the unit cell.

Calculation of the macroscopic properties of the unit cell are dictated by first calculating the properties of the constituent elements and averaging accurately the contribution they make to a macroscopic layer and subsequently the whole unit cell. Various authors analytical approaches accepted highly idealised representation of tow cross-sectional shape. For example Tan et. al.[10] presented the *XYZ*, *ZXY* and *ZYX* models to predict the stiffness of 3D woven composites. The representative unit cell was segmented into a number of micro-blocks where the authors proposed a mixed iso-strain and iso-stress scheme to calculate the elastic properties of the 3D woven composite. These microblocks could be resin impregnated stuffer, filler or binder tow blocks where the cross-sectional shape of the tow was taken to be rectangular.

Utilising non-representative tow cross-sectional characteristics could lead to inaccurate calculation of volume fraction at the tow element level. This is compounded further when calculating the volume fraction of the respective elements that make up a layer in the unit cell. The highly idealised representation of the geometric characteristics of the constituent parts (stuffers, fillers, binders and matrix) that make up a layer must be improved in order to yield better predictions. Existing analytical models[8-11,13,17] present predictions that are generally significantly higher, by 10% compared to the small amount experimental data available in literature.

This paper presents an analytical modelling tool to predict the elastic stiffness properties of 3D woven orthogonal interlock composites. The model assesses the change in performance as a consequence of altering the weaving parameters that dictates the 3D weave architecture. The 3D woven composite modelled in this paper consists of alternate layers of stuffers travelling in the 0^o (warp) direction and fillers travelling in the 90^o (weft) direction bound through-the-thickness in the warp direction by a binding tow (Figure 1).

Previous work by Buchanan et. al.[18] describe the development of a geometric model that is capable of calculating the necessary inputs for the present elastic stiffness model. The geometric model and the present elastic stiffness model are driven by weaving parameters and the constituent material properties from the manufacturer's datasheet. The modelling methodology from the geometric model predicts useful information for the engineer such as areal density, overall thickness and fibre volume fraction in addition to the variables that appear in equations 8 to 16 of this paper. The geometric model also defines the composite unit cell to be modelled by the elastic stiffness model, accepting more representative tow cross-sectional characteristics. The geometric model allowed three representative tow cross-sectional shapes to be used including lenticular, elliptical and racetrack. A racetrack cross section is essentially a rectangle with semi-circles on its ends. Assumption of any of these tow cross sectional shapes is still an idealisation. For instance Summerscales and Russell[19] found evidence that assuming the lenticular shape to be symmetrical is incorrect. However, one or more of these ideal tow cross sections is often adopted in models[18,20-22] and have shown good agreement between calculated and measured values.

The macroscopic unit cell modelled by the present elastic stiffness model is representative of one repeat of the weave architecture (Figure 1). The model follows the unit cell discretisation method into layers and elements. Elements within a layer can be pure matrix material, or a combination of reinforcing tows in the X or Y, and Z axis directions. The present approach formulates expressions at the micro level with the aim of calculating more representative volume fractions of a group of elements to the layer. The rationale in representing the volume fractions of elements within a layer and subsequently the layers within the unit cell more accurately was to improve the elastic stiffness predictions compared with existing analytical modelling approaches for example Cox and Dadkhaha[8] and Wu et. al.[13].

2. Description of present modelling approach

The modelling approach taken in this paper follows from Naik et. al.[11,17] and develops the modelling approach by Wu et. al.[13]. The unit cell in this work is representative of one repeat of the weave architecture. The new model treats the 3D woven composite as an assembly consisting of layers containing unidirectional elements (which are fibrous tows encased in resin). The new modelling approach formulates expressions that discretise the unit cell into layers and then elements.

Figure 2 illustrates the operation of the elastic stiffness model. Upon execution of elastic stiffness model the geometric properties originating from the results provided by the geometric modelling methodology[18] selects the unit cell to be discretised. The whole unit cell is representative of the macroscale i.e. does not distinguish individual layers nor the elements that make up a layer. To

calculate the macroscopic stiffness of the whole unit cell it must be broken down or discretised to the microscale. The microscale looks at the individual elements that make a layer and then the layers that make up the macroscopic unit cell. Therefore, the unit cell undergoes the first level discretisation into layers then the 2nd level discretisation into the individual elements that make up the layer. An element can be an individual stuffer, filler, binder or matrix region within a layer. At this stage the micro stiffness of the each individual element contained within a layer is calculated. Having determined the stiffness of each and every element then the stiffness of whole layers can be calculated following the procedure discussed in section 3.2. A layer within the unit cell can be an outermost layer (figure 3), a warp layer oriented in the *X* direction (figure 5) or weft layer oriented in the *Y* direction (figure 4). Once the stiffness of all layers is known then the model calculates the stiffness of the whole unit cell and finally outputs the elastic constants following the procedure discussed in section 3.1. The predictions of the elastic constants are compared with the experimental data and two existing analytical models, the Orientation Averaging (OA) and Modified Orientation Averaging (MOA) and an FE model (binary model) that are reported in literature by Cox and Dadkhaha[8] and Xu et. al.[23] respectively. In addition, the present approach is compared with the analytical model presented by Wu et. al.[13] for 3D woven orthogonal interlock composites.

3. Formulation of elastic stiffness model

The prediction of the unit cell or macroscopic stiffness begins with the calculation at the microscale i.e. the constituent elements within a layer. At this level the constituent elements (tows encased in matrix) are considered to be unidirectional composites. The micromechanical equations described by Chamis[24] have been used elsewhere[13] to calculate the effective the elastic properties of the element on the material coordinate system i.e. 1, 2, 3. Direction 1 coincides with the longitudinal direction of the tow, transverse direction with 2 and out-of-plane with 3 (figure 6).

The volume fraction (V_o) of a tow element is calculated from the characteristic dimensions of the tow and the unit cell that were predicted previously by the geometric model[18]. The V_o of the tow is equal to the area fraction of the tow and is determined via equation 1. V_o is the total cross sectional area of the individual filaments in a tow divided by the area of a rectangular prism of resin (*i = s*, *f* and *b* *stuffer*, *filler* and *binder*). The cross sectional area of a tow was determined from the respective linear density (TEX) and density of the fibre with an assumed packing factor(see Buchanan et. al [18]).

$$V_o = \frac{A_i}{h_i l_i} \qquad \textbf{Eq 1}$$

Where:

A_i = Cross sectional area of the tow (calculated by geometric model[18])

h_i = height of the tow (calculated by geometric model[18])

l_i = width of the tow (calculated by geometric model[18])

With the proportions of the constituent composite parts and the elastic modulus supplied from the manufacturer's data, the stiffness of the unidirectional tow/element is calculated by the model using equations 2 to 7. The reinforcing tows are assumed to be transversely isotropic and the matrix is isotropic.

Elastic moduli [24]*:*

$$E_1 = E_{f1}V_o + E_m(1 - V_o) \quad \textbf{Eq 2}$$

$$E_2 = E_3 = \frac{E_m}{\left[1 - \sqrt{V_o}\left(1 - E_m / E_{f2}\right)\right]} \quad \textbf{Eq 3}$$

Shear moduli [24]*:*

$$G_{12} = G_{21} = \frac{G_m}{\left[1 - \sqrt{V_o}\left(1 - G_m / G_{f12}\right)\right]} \quad \textbf{Eq 4}$$

$$G_{23} = G_{13} = \frac{G_m}{\left[1 - \sqrt{V_o}\left(1 - G_m / G_{f23}\right)\right]} \quad \textbf{Eq 5}$$

Poisson ratio[24]*:*

$$\upsilon_{12} = \upsilon_{13} = \upsilon_{f12}V_o + \upsilon_m(1 - V_o) \quad \textbf{Eq 6}$$

$$\upsilon_{23} = \frac{E_2}{2G_{23}} - 1 \quad \textbf{Eq 7}$$

Described next are the expressions that describe the discretisation of the 3D woven orthogonal interlock unit cell into layers and the calculation of the contribution that each element makes to the respective layer. Calculation of element contribution is required so that the stiffness of the whole layer can be calculated and ultimately the overall unit cell stiffness. The input data for the specific 3D woven orthogonal interlock type modelled in this paper is found in Cox et. al.[8] and Wu et. al.[13]. This enables the present modelling approach to be compared to existing models in literature in addition to experimental data.

The outer most layers contain horizontal and vertical binder tow elements and resin material only. The horizontal binder elements illustrated in Figure 1 are where the binder tow emerges to the surface looping over a number of filler tows (the float length *F* dictated by the weave design) before passing down through the thickness of the unit cell. The derivation and calculation of the variables in equations 8 to 16 are found elsewhere in Buchanan et. al.[18]

Contribution of horizontal binder elements in the outer layer $V_{bhOUTER}$:

$$V_{bhOUTER} = \frac{n_b{}^{uc}\left(\frac{C_f}{2}\right)A_b + F.AR_f h_f A_b}{L_x L_y h_b} \quad \textbf{Eq 8}$$

- The in-plane contribution of the binder elements in the outer layer $V_{bvOUTER}$:

$$V_{bvOUTER} = \frac{n_b{}^{uc}\left(\frac{C_f}{2}\right)A_b}{L_x L_y h_b} \quad \textbf{Eq 9}$$

- Contribution of matrix elements V_{mOUTER} :

$$V_{mOUTER} = 1 - \left(V_{bh} + V_{bv}\right) \quad \textbf{Eq 10}$$

2. Intermediate/inner layers

Intermediate layers are either weft layers or warp layers that alternate weft/warp from top to bottom.

- **Weft layers:**

Contain straight filler elements, vertical elements of binder tows and matrix material elements. An example of this is illustrated in Figure 4.

The contribution of each element in the weft layer is as follows:

- Contribution of vertical binder elements in a weft layer V_{bvWEFT} :

$$V_{bvWEFT} = \frac{2n_b{}^{uc}A_b}{L_x L_y} \quad \textbf{Eq 11}$$

- Contribution of filler tow elements in a weft layer V_{fWEFT} :

$$V_{fWEFT} = \frac{n_f{}^{uc}A_f}{L_x h_f} \quad \textbf{Eq 12}$$

- Contribution of matrix elements in a weft layer V_{mWEFT}:

$$V_{mWEFT} = 1 - \left(V_{bh} + V_f\right) \quad \textbf{Eq 13}$$

- **Warp layers :**

Contain stuffers, vertical binders and matrix material an example is illustrated in Figure 5.

The contribution of each element in the warp layer is as follows:

- Contribution of vertical binder elements in a warp layer V_{bvWARP}:

$$V_{bvWARP} = \frac{2n_b{}^{uc} A_b}{L_x L_y} \quad \textbf{Eq14}$$

- Contribution of stuffer tow elements in a warp layer V_{sWARP}:

$$V_{sWARP} = \frac{n_s{}^{uc} A_s}{L_y h_s} \quad \textbf{Eq 15}$$

- Contribution of matrix elements V_{mWARP}:

$$V_{mWARP} = 1 - \left(V_{bh} + V_s\right) \quad \textbf{Eq 16}$$

a. Determination of the elastic properties of the unit cell

On the macro-scale or unit cell level the composite is homogenous and orthotropic and is characterised via the following constitutive relationship:

$$\sigma = C.\varepsilon \quad \textbf{Eq 17}[25]$$

$$\varepsilon = S.\sigma \quad \textbf{Eq 18}[25]$$

Where:

σ: macrostress vector

ε: macrostrain vector

C: macroscale orthotropic elastic stiffness matrix

S: macroscale orthotropic elastic compliance matrix

This is a linear stress-strain relationship that is given by a six-by-six stiffness and compliance matrices *C* and *S* respectively (generalised Hooke's law). The assumption of material orthotropy considers the composite material to possess three mutually orthogonal planes of symmetry.

The objective is to determine the macroscale elastic stiffness matrix *C*, which is the overall stiffness of the unit cell. This is formulated by considering microscale response of the individual elements in the layers that make up the unit cell i.e. the discretisation of the unit cell. The elements are treated as spatially orientated unidirectional composites. Where, considering the global material axis (X, Y, Z) - the stuffer and horizontal binder elements flow in the X-axis, filler elements in the Y-axis and vertical binder elements in the Z-axis. The elastic stiffness of the respective elements C^e and compliance S^e as a consequence of their spatial orientation is specified by the matrix transformation of an orthotropic matrix:

$$\overline{C^e} = T.C^e.T^{-T} \text{ [26]}$$

$$\overline{S^e} = T^T.S^e.T \text{ [26]}$$

Where:

$\overline{C^e}$ and $\overline{S^e}$ = the transformed stiffness and compliance matrix respectively

T = the transformation matrix superscript ^{T} indicates the transpose of *T*

By calculating the stiffness C^l and compliance S^l of every layer by applying isostrain or isostress conditions and considering the volume fraction of the layer then the overall macroscopic stiffness *C* can be determined based on the generalised Hooke's law (assuming the unit cell is orthotropic). The isostrain (stiffness) condition is applied when determining the elastic stiffness predictions in the fibre direction and the isostress (compliance) condition is applied for predictions transverse to the fibre direction. This is because it has been found that for unidirectional composites the isostrain conditions provide better predictions in the fibre direction and isostress is better for calculation transverse properties[27].

Considering equation 17 in matrix form and a considering a stress applied in the longitudinal X direction results:

$$\begin{Bmatrix} \sigma_x \\ 0 \\ 0 \end{Bmatrix} = \begin{bmatrix} C_{11} & C_{12} & C_{13} \\ C_{12} & C_{22} & C_{23} \\ C_{13} & C_{23} & C_{33} \end{bmatrix} . \begin{Bmatrix} \varepsilon_x \\ \varepsilon_y \\ \varepsilon_z \end{Bmatrix} \qquad \textbf{Eq 19}$$

Equation 19 illustrated the macroscale response which is to be determined by summation of the stress distributions within a layer *l* :

$$\begin{Bmatrix} \sigma^l{}_x \\ \sigma^l{}_y \\ \sigma^l{}_z \end{Bmatrix} = \begin{bmatrix} C^l{}_{11} & C^l{}_{12} & C^l{}_{13} \\ C^l{}_{12} & C^l{}_{22} & C^l{}_{23} \\ C^l{}_{13} & C^l{}_{23} & C^l{}_{33} \end{bmatrix} . \begin{Bmatrix} \varepsilon^l{}_x \\ \varepsilon^l{}_y \\ \varepsilon^l{}_z \end{Bmatrix} \qquad \textbf{Eq 20}$$

Assuming:

$$\varepsilon_x = \varepsilon^l{}_x \ , \ \varepsilon_y = \varepsilon^l{}_y \qquad \textbf{Eq 21}[13]$$

Equations 5-22 mean that the macroscopic strain experienced by the unit cell is equal to the strain experienced by each individual layer *l.*

$$\varepsilon_z = \sum_l \frac{h_l}{H} \varepsilon^l{}_z \qquad \textbf{Eq 22}[13]$$

Where, a layer *l* (1, 2, 3, n) and the thickness of a layer is denoted as h_l and *H* is the overall thickness of the unit cell.

Equation 22 indicates that the strain Through-The-Thickness (T-T-T) of the unit cell is equal to the summation of all individual T-T-T strains experienced by the layers in the unit cell.

For the assumption that the unit cell is in equilibrium requires the following expressions:

$$\sigma_x = \sum_l \frac{h_l}{H} \sigma^l{}_x \qquad \textbf{Eq 23}[13]$$

$$0 = \sum_l L_x h_l \sigma^l{}_y \qquad \textbf{Eq 24}[13]$$

Plane stress condition applies to the layer, as such:

$$\sigma^l{}_z = 0 \qquad \textbf{Eq 25}[13]$$

Applying these assumptions and isostrain and isostress conditions results in expressions (Table 1) describing the elastic constants of the unit cell in terms of the elastic stiffness of the layers. The procedure to find the elastic constants for the overall unit cell is the same as detailed by Wu et. al. [13] and repeating the procedure whilst considering deformation or strain to the unit cell in the transverse Y direction yields the expressions in Table 1.

The simplified variables in Table 1 are representative of the following expressions:

$$\sum_l \frac{h_l}{H}\left(C^l{}_{11} - \frac{C^l{}_{13}{}^2}{C^l{}_{33}} \right) = C_1 \ , \ \sum_l \frac{h_l}{H}\left(C^l{}_{22} - \frac{C^l{}_{23}{}^2}{C^l{}_{33}} \right) = C_2 \ , \ \sum_l \frac{h_l}{H}\left(C^l{}_{12} - \frac{C^l{}_{13}.C^l{}_{23}}{C^l{}_{33}} \right) = C_3 \ ,$$

$$\sum_l \frac{h_l}{H}\frac{C^l{}_{13}}{C^l{}_{33}} = C_4 \ , \ \sum_l \frac{h_l}{H}\frac{C^l{}_{23}}{C^l{}_{33}} = C_5$$

b. Determination of the elastic stiffness of the layers and elements

By applying isostrain/isostress conditions to the layer the same procedure that has just been described to determine the overall stiffness and compliance matrices *C* and *S* and layer stiffness and compliance matrices C^l and S^l, can also be expressed for C^l and S^l and C^e and S^e. The determination of element volume fractions is different than the volume fraction of a layer such that h_l/H must be

replaced in the expressions by V_e/V for warp, weft and outer layers. Then by replacing the assumptions described in Equations 22-25 with 32-35 the stiffness properties of individual layers in the unit cell can be determined. A layer consists of a number of elements e_n where subscript n dictates the number of the element in the layer (Figure 6). The calculation of the stiffness of the individual layers must be carried out first so that the stiffness of the whole unit cell can be determined.

The deformation of the layer in the longitudinal direction X results in:

$$\begin{Bmatrix} \sigma^{l}{}_{x} \\ 0 \\ 0 \end{Bmatrix} = \begin{bmatrix} C^{l}{}_{11} & C^{l}{}_{12} & C^{l}{}_{13} \\ C^{l}{}_{12} & C^{l}{}_{22} & C^{l}{}_{23} \\ C^{l}{}_{13} & C^{l}{}_{23} & C^{l}{}_{33} \end{bmatrix} . \begin{Bmatrix} \varepsilon^{l}{}_{x} \\ \varepsilon^{l}{}_{y} \\ \varepsilon^{l}{}_{z} \end{Bmatrix} \quad \textbf{Eq 26}$$

The elastic response of the whole layer is to be determined by summation of the stress distributions of the elements *e* within a layer *l*:

$$\begin{Bmatrix} \sigma^{e}{}_{x} \\ \sigma^{e}{}_{y} \\ \sigma^{e}{}_{z} \end{Bmatrix} = \begin{bmatrix} C^{e}{}_{11} & C^{e}{}_{12} & C^{e}{}_{13} \\ C^{e}{}_{12} & C^{e}{}_{22} & C^{e}{}_{23} \\ C^{e}{}_{13} & C^{e}{}_{23} & C^{e}{}_{33} \end{bmatrix} . \begin{Bmatrix} \varepsilon^{e}{}_{x} \\ \varepsilon^{e}{}_{y} \\ \varepsilon^{e}{}_{z} \end{Bmatrix} \quad \textbf{Eq 27}$$

Assuming:

$$\varepsilon^{l}{}_{x} = \varepsilon^{e}{}_{x} \ , \ \varepsilon^{l}{}_{z} = \varepsilon^{e}{}_{z} \quad \textbf{Eq 28}[13]$$

Equations 28 mean that the strain experienced by the layer *l* is equal to the strain experienced by each element *e*.

$$\varepsilon^{l}{}_{y} = \sum_{e} \frac{V_e}{V} \varepsilon^{e}{}_{y} \quad \textbf{Eq 29}$$

Where:

V_e can be the volume of a stuffer, filler or binder element depending on the layer and V is the volume of the layer. V_e for each respective element was detailed earlier for each respective layer (Equations 8 to 16). This differs from the approach reported by Wu et. al. [13] who calculated volume fraction of an element based on element width.

Equation 29 indicates the transverse strain in the whole layer is equal to the summation of all individual element strains in the layer.

For the assumption that the unit cell is in equilibrium requires the following expressions:

$$V\sigma_x{}^{l} = \sum_e V_e.\sigma^e{}_x \qquad \textbf{Eq 30}$$

$$0 = \sum_e \frac{V_e}{V}.\sigma^e{}_y \qquad \textbf{Eq 31}$$

$$0 = \sum_e \frac{V_e}{V}.\sigma^e{}_z \qquad \textbf{Eq 32}$$

Following a similar procedure as before to calculate the elastic stiffness constants of the unit cell, the elastic stiffness constants of the layer can be determined (Table 2).

The simplified variables in Table 2 are representative of the following expressions:

$$\sum_e \frac{V_e}{V}\left(C^e{}_{11} - \frac{C^e{}_{12}{}^2}{C^e{}_{22}}\right) = C_{1e}, \quad \sum_e \frac{V_e}{V}\left(C^e{}_{33} - \frac{C^e{}_{23}{}^2}{C^e{}_{22}}\right) = C_{2e}, \sum_e \frac{V_e}{V}\left(C^e{}_{13} - \frac{C^e{}_{12}.C^e{}_{23}}{C^e{}_{22}}\right)^2 = C_{3e},$$

$$\sum_e \frac{V_e}{V}\frac{C^l{}_{12}}{C^l{}_{22}} = C_{4e}, \qquad \sum_e \frac{V_e}{V}\frac{C^l{}_{23}}{C^l{}_{22}} = C_{5e}$$

4. Results and Discussion

Table 3 indicates the predictions from present model compared to the experimental data and two analytical models reported by Cox and Dadkhaha[8], a numerical model by Xu et. al.[23] and the predictions of another analytical model that are stated by Wu et. al. [13].

The results show that the new modelling approach has a clear improvement in all predictions compared to both the Orientation Averaging (OA) and Modified Orientation Averaging (MOA) models. The predictions made by the present model are more accurate than those made by the binary model with the exception of the T-T-T modulus E_z. The same is also true when comparing the analytical model by Wu et. al.[13], where more accurate predictions for longitudinal and transverse modulus and Poisson's ratio are achieved by the present model. The binary model and Wu et. al.'s model appear to produce a slightly better prediction for T-T-T modulus E_z than the present model. However, the experimental value for E_z was implied from a compression test T-T-T of the laminate and may not be accurate with a deviation of ±1GPa. In all predictions the percentage difference between the present modelling predictions and experimental data for E_x, E_y, E_z and υ_{xy} are 12.87%, 4.91%, 36.82% and 32.5% respectively. The overestimation of E_z in the present model is most likely the assumption that orthogonal binder tow path passes perpendicularly T-T-T. In practice the binder folds on itself as a consequence of consolidation in the moulding process that alters its trajectory T-T-T.

The MOA is more accurate than its predecessor the OA model because waviness measurements were taken for the nominally straight stuffer and fillers tows and found to be 0.86 and 0.98 respectively[8]. This implies stuffer tows possessed more undulation than filler tows that could be

considered to be nominally straight (1 is indicative of a completely straight tow). The predictions made in the present model do not require any such measurements and still yield better predictions. Although, the E_x is overestimated by present model by a larger percentage than E_y, this can be explained by the fact that the filler tows that contribute most to E_y are nominally straight but the stuffers that contribute most to E_x are more undulated. Undulation in the nominally straight tows was reported by the Cox and Dadkhaha[8] to result in a knock-down in elastic stiffness. The results found in this research support the role of undulation and its importance that it is incorporated into further modelling efforts especially for 3D weaves that possess a lot of undulation in the nominally straight tows. However, the present modelling approach identifies this as only part of the solution. Because the present model more accurately accounts for the volume fractions of the elements at the micro level and selects a unit cell representative as one repeat of the weave architecture, more accurate predictions are achieved. Therefore, accurate calculation of fibre volume fractions is crucial for calculating the in-plane properties that have been reported by Tan et. al.[28] to be 'highly sensitive' to fibre volume fraction. Also, it may be implied from the predictions made by the present model that if the undulation factor is not less than 0.9 (less meaning greater undulation) then the in-plane modulus can be predicted to within 10% of the experimental value.

5. Conclusions

- A new analytical tool has been presented to model the elastic stiffness characteristics of 3D woven orthogonal composites with the ability to assess change in performance as a consequence of altering weaving parameters.
- The elastic stiffness model discretises the unit cell into layers and subsequently elements. New expressions have been presented and incorporated into the model to calculate more accurately the volume fractions of constituent elements in a layer. This approach has been validated against experimental data produced independently of this work for orthogonal interlock weaves and compared to existing modelling approaches.
- The present model performs better in all predictions compared to the existing modelling efforts except for the prediction of E_z.
- The representation of the trajectory of the binding tow in orthogonal interlock weaves is too idealised in the present model. It is assumed to pass perpendicular through the whole thickness of the laminate resulting in overestimated predictions for E_z.
- Undulation in the nominally straight stuffer and filler tows negatively affects the accuracy of the predicted results.
- For tow undulation factors ≥0.9 the present model will predict longitudinal or transverse modulus to within 10%.

Abbrevations

2D	Two-Dimensional

3D	Three-Dimensional
FE	Finite Element
MOA	Modified Orientation Averaging
OA	Orientation Averaging
T-T-T	Through-The-Thickness

Symbols

A	Area (m^2)
AR	Aspect Ratio of the tow cross-section
C_f	Circumference of filler tow (m)
C_{ij}	Orthotropic stiffness matrix
E	Modulus of elasticity (GPa)
F	Float (orthogonal interlock only) number of fillers binder travels over
G	Shear modulus (GPa)
h	Thickness of a tow (m)
H	Thickness of unit cell (m)
l	Length a tow (m)
L	Length of unit cell (m)
n_s^{uc}	Number of stuffers along the weft direction (Y) in the unit cell
n_f^{uc}	Number of fillers along the warp direction (X) in the unit cell
n_b^{uc}	Number of binders along the weft direction (Y) in the unit cell
S_{ij}	Orthotropic compliance matrix
T	Transformation matrix
V	Volume (m^3)
V_m	Volume fraction of a matrix

V_o	Volume fraction of a tow

Greek letters

ε	Strain
v	Poisson's ration
σ	Stress (GPa)

Subscript

1	Longitudinal fibre direction (material co-ordinate system)
2	Transverse fibre direction (material co-ordinate system)
3	Transverse fibre direction (material co-ordinate system)
bv	Vertical binder element
bh	Horizontal binder element
b	Binder tow
e	Element
f	Filler tow
l	Layer
OUTER	Outer layer in the unit cell
s	Stuffer tow
WARP	Warp layer in the unit cell
WEFT	Weft layer in the unit cell
x	in the longitudinal *x* axis

y	in the transverse y axis
z	in the out-of-plane *z* axis

Superscript

-1	Inverse of matrix
e	element
l	Layer
T	Transpose of matrix

References

1. Mouritz AP, Bannister MK, Falzon PJ, Leong KH. Review of applications for advanced 3-dimensionally fibre textile composites. Composites Part A: Applied Science and Manufacturing 1999;30:1445-1461.

2. Dickinson L, Salama M, Stobbe D. Design Approach for 3D Woven Composites: Cost vs Performance. 46th International SAMPE Symposium 2001.

3. Mouritz A.P. A Simple Fatigue Life Model for Three-Dimensional Fiber-Polymer Composites. Journal of Composite Materials 2006;40:455-469.

4. Cox BN, Dadkhah MS, Morris WL. On the tensile failure of 3D woven composites. Composites Part A: Applied Science and Manufacturing 1996;27(6):447-458.

5. Brandt J, Drechsler K, Arendts FJ. Mechanical performance of composites based on various three-dimensional woven-fibre preforms. Composites Science and Technology 1996;56(3):381-386.

6. Bogdanovich AE, Mohamed MH. Three dimensional reinforcements for composites. SAMPE Journal 2009;45(6):8-28.

7. Pelegri AA, Kedlaya DN. Design of composites using a generic unit cell model coupled with a hybrid genetic algorithm. Composites Part A: Applied Science and Manufacturing 2008;39:1433-1443.

8. Cox BN, Dadkhaha MS. The macroscopic elasticity of 3D woven composites. Journal of Composite Materials 1995;29:785-819.

9. Tan P, Tong L, Steven GP. Modelling approaches for 3D orthogonal woven composites. Journal of Reinforced Plastics and Composites 1998;17:545-577.

10. Tan P, Tong L, Steven GP. Micromechanics models for mechanical and thermo-mechanical properties of 3D through-the-thickness interlock woven composites. Composites Part A: Applied Science and Manufacturing 1999;30:637-648.

11. Naik NK, Azad NM, Prasad DP. Stress and failure analysis of 3D angle interlock woven composites. J Composite Mater 2002;36:93-123.

12. Naik NK, Sridevi E. An analytical method for thermoelastic analysis of 3D orthogonal interlock woven composites. Journal of Reinforced Plastics and Composites 2002;21:1150-1188.

13. Wu ZJ, Brown D, Davis JM. An analytical modelling technique for predicting the stiffness of 3D orthotropic laminated fabric composites. Composite Structures 2002;56:407-412.

14. Yanjun C, Guiqiong J, Bo W, Wei L. Elastic behavior analysis of 3D angle-interlock woven ceramic composites. Acta Mechanica Solida Sinica 2006;19:152-159.

15. Nicosia MA, Vineis F, Lawrence J, Holmes AT. Microstructural modelling of three-dimensional woven fiber composites. Proceedings of the 9th International Conference on Textile Composites (Texcomp9) 2008;VI:264-271.

16. Lomov SV, Belov EB, Verpoest I. Integrated models of textile composites. High performance structures and composites 2002;59:481-490.

17. Naik NK. An analytical model for the thermoelastic analysis of 3D orthogonal interlock woven composites. Journal of Reinforced Plastics and Composites 2002;21:1150-1191.

18. Buchanan S, Grigorash A, Quinn JP, McIlhagger AT, Young C. Modelling the geometry of the repeat unit cell of three-dimensional weave architectures. Journal of the Textile Institute 2009;First Published on: 17th November 2009 (iFirst):1-7.

19. Summerscales J, Russell PM. Observations on the fibre distribution and fibre strain in a woven fabric reinforcement. Advanced Composite Letters 2004;13(3):135-140.

20. Quinn JP, McIlhagger R, McIlhagger AT. A modified system for design and analysis of 3D woven preforms. Composites Part A: Applied Science and Manufacturing 2003;34:503-509.

21. Morgan M. Geometric modelling of 3D woven reinforcements in composite materials. PhD Dissertation 2005:15-31.

22. Brown D, Wu ZJ. Geometric modelling of orthogonal 3D woven textiles. International Conference for Manufacturing of Advanced Composites 2001:52-65.

23. Xu J, Cox BN, McGlockton MA, Carter WC. A binary model of textile composites -II. The elastic regime. Acta Metallurgica et Materialia 1995;43:3511-3524.

24. Chamis CC. Simplified composite micromechanics equations for hygral, thermal, and mechanical properties. SAMPE Quarterly 1984(April):14-23.

25. Jones RM. Stiffness, Compliances, and engineering constants for orthotropic materials. In: Taylor Francis, editor. Mechanics of Composite Materials, 1998.

26. Jones RM. Stress-strain relations for a lamina of arbitrary orientation. In: Taylor Francis, editor. Mechanics of Composite Materials, 1998.

27. Bogdanovich AE. Three-dimensional continuum micro-, meso- and macro-mechanics of textile composites. TEXCOMP-8 2006:T56-1 - T56-13.

28. Tan P, Tong L, Steven GP. Modelling for predicting the mechanical properties of textile composites - A review. Composites Part A: Applied Science and Manufacturing 1997;28A:903-922.

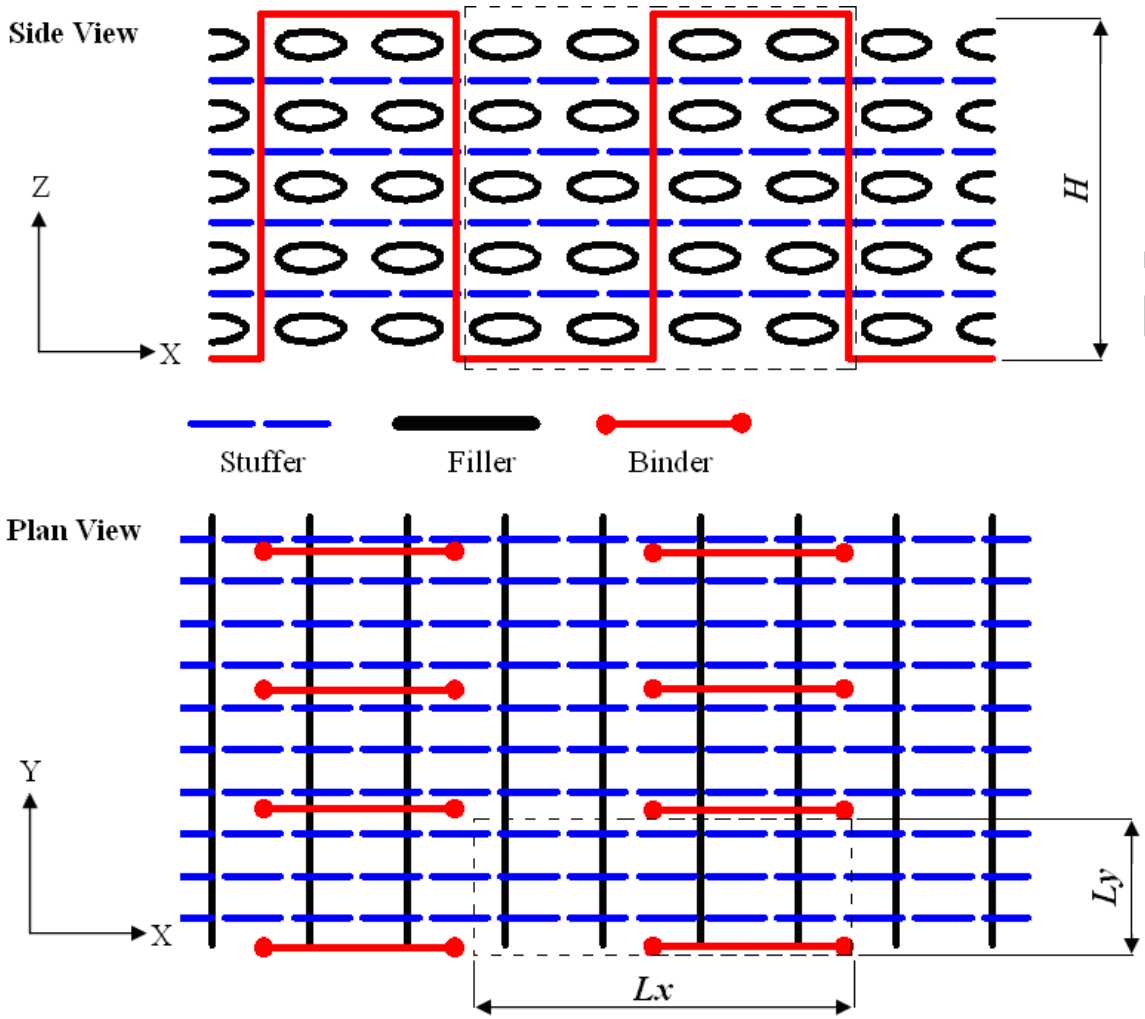

Figure 1: Schematic representation of 3D woven orthogonal interlock type

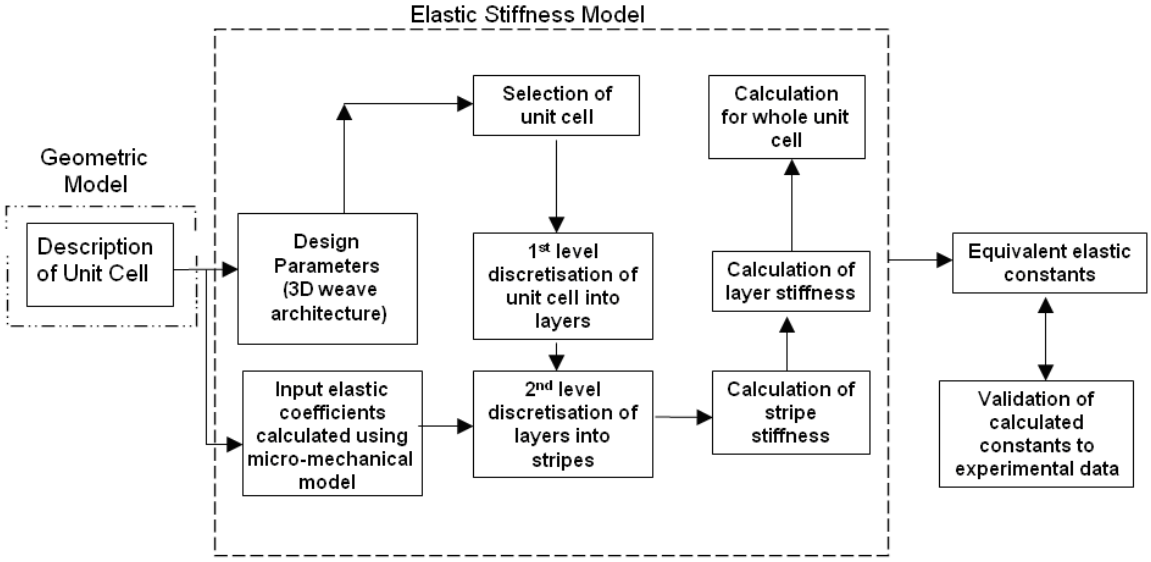

Figure 2: Model flowchart

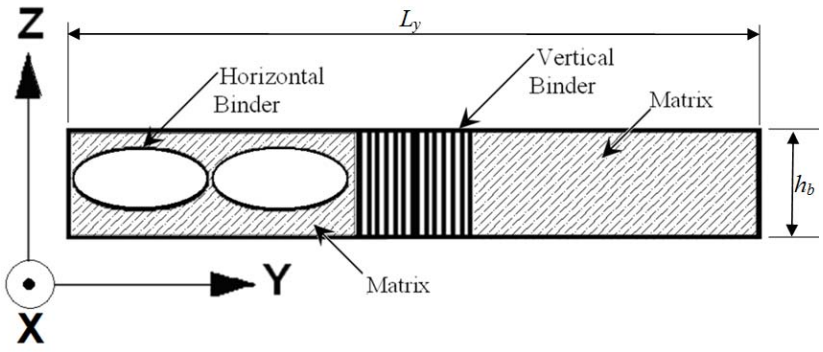

Figure 3: Outer layer of unit cell

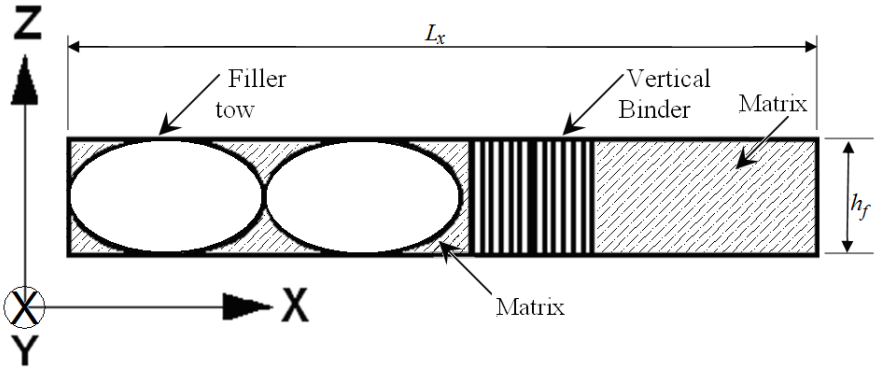

Figure 4: Schematic representation of intermediate weft layer

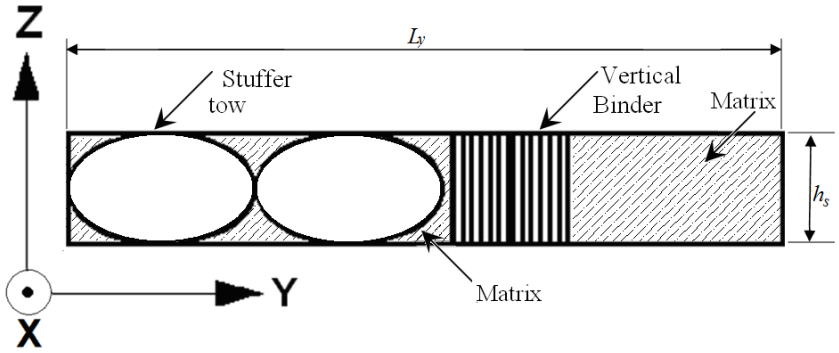

Figure 5: Schematic representation intermediate warp layer (orthogonal interlock)

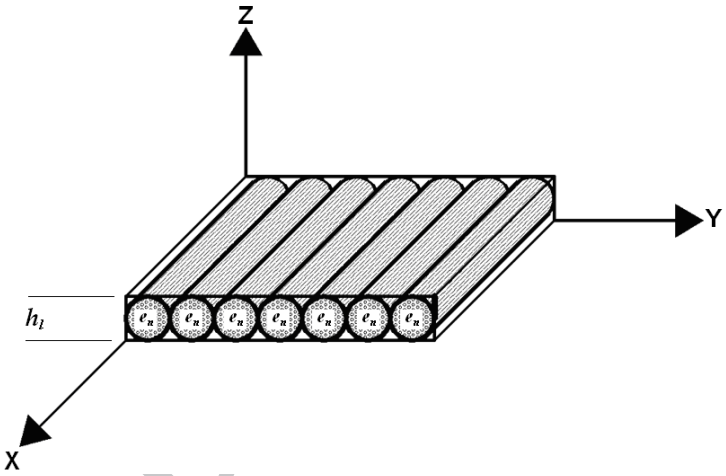

Figure 6: Layer containing stripes on the global co-ordinate system

Table 1: Elastic constants for the unit cell

Elastic constant	Expression
C_{11}	$C_1 + C_4{}^2 C_{33}$
C_{12}	$C_3 + C_4 C_5 C_{33}$
C_{13}	$C_4 . C_{33}$
C_{23}	$C_2 + C_5{}^2 . C_{33}$
C_{22}	$C_5 . C_{33}$
C_{33}	$-\frac{C_1 C_2 - C_3{}^2}{C_2 C_4{}^2 + C_4 C_5{}^2 - 2 C_3 C_4 C_5}$

Table 2: Elastic constants for the layers

Elastic constant	Expression
$C_{11}{}^l$	$C_{1e} + C_{4e}{}^2 C_{22}{}^l$
$C_{12}{}^l$	$C_{4e} . C_{22}{}^l$
$C_{13}{}^l$	$C_{3e} + C_{4e.} C_{5e} . C_{22}{}^l$
$C_{23}{}^l$	$C_{5e} . C_{22}{}^l$
$C_{22}{}^l$	$-\frac{C_{1e} C_{2e} - C_{3e}{}^2}{C_{1e} C_{5e}{}^2 + C_{2e} C_{4e}{}^2 - 2 C_{3e} C_{4e} C_{5e}}$
$C_{33}{}^l$	$C_{2e} + C_{5e}{}^2 . C_{22}{}^l$

Table 3: Elastic stiffness predictions for 3D woven orthogonal interlock compared to experimental data

Models	E_x (GPa)	E_y (GPa)	E_z (GPa)	υ_{xy}	υ_{yz}	υ_{xz}
OA (Cox et al[8])	51.90	63.90	13.70	0.034	0.183	0.184
MOA (Cox et al[8])	45.40	62.60	13.70	0.032	0.180	0.173
Binary Model (Xu et al[23])	48.90	63.70	9.40	0.027	0.428	-
Analytical Model (Wu et al[12])	45.30	55.90	8.90	0.031	0.205	0.207
Present model	**34.43**	**47.85**	**11.08**	**0.040**	**0.211**	**0.201**
Experimental	30.00±2.0	45.50±1.5	7.0±1.0	0.053	-	-
Error between present model and experiment	*12.87%*	*4.91%*	*36.82%*	*32.50%*	-	-